Supplementary Information (SI) for Journal of Materials Chemistry A.
This journal is © The Royal Society of Chemistry 2026

–Supporting information–
Solvation Effect on the Electrocatalytic Nitrogen Reduction Reaction: A Deep Potential Molecular Dynamics Simulation with Enhanced Sampling for the Case of the Ruthenium Single Atom Catalyst

Bowen Zhang[1], **Pengchao Zhang**[1], and **Xuefei Xu**[1,*].

[1]Center for Combustion Energy, Department of Energy and Power Engineering, and Key Laboratory for Thermal Science and Power Engineering of Ministry of Education, Tsinghua University, Beijing 100084, China

[*]Corresponding author e-mail: xuxuefei@tsinghua.edu.cn

December 19, 2025

Contents

Additional details of DFT calculations

All DFT structural optimizations and energy calculations were performed using the CP2K package.[1] In single-point calculations for generating a large-scale training set, the magnetization used in the atomic initial guess was assigned to the C, N, O, and H elements as follows: 0.6, 1, 0.6, and 0.6, respectively. Notably, specifying an appropriate initial magnetization for the Ru atom significantly improved the convergence of energy for the current systems. An initial magnetization of 5 for Ru worked for most of structures; however, for some configurations involved in the target reactions R1 and R2, an initial magnetization of 3 was set up for Ru to improve the convergency.

Additional details of CHE model calculations

In the free energy calculations using the CHE model,[2] the needed frequency information of the optimized structures are obtained by allowing the atoms of adsorbate species to relax with the catalyst fixed at their optimized geometries. For the frequency calculations of small gas molecules, like N_2 and H_2, all atoms are allowed to move freely. Thermodynamic quantities are calculated at 300 K and an atmospheric pressure. For adsorbate species, only vibrational contributions are considered in the thermodynamic calculations; however, for gas-phase small molecules, contributions from translational, rotational, and vibrational modes are taken into account. The results of energy and the corresponding Gibbs free energy correction (ΔG_{corr}) are listed in Tab. S1. The asterisk (*) indicates that the species after the asterisk is adsorbed on the Ru-N_4-C catalyst.

Table S1: The energy E and the corresponding Gibbs free energy correction (ΔG_{corr}) calculated for some key species.

structure	E (Hartree)	ΔG_{corr} (Hartree)
Ru-N4-C (*)	-441.990732	-
*NN	-461.944473	0.004642
*NNH	-462.490794	0.013726
*H	-442.609409	0.00674
H_2	-1.1619256	0.000031
N_2	-19.895060	-0.013135

Additional details of DP model training

The DP model was trained following the active-learning approach of Zhang et al.[3–5] The descriptor of "se_e2_a" is used where the embedding net size is set to [25, 50, 100] per layer and the non-linear activation function between hidden layers is "tanh". The submatrix size in the embedding net is set to 16. A neighbor atom cutoff radius of 6.0 Å with smoothing beginning at 0.5 Å is used. The fitting net is connected after the embedding net, with a size of [240, 240, 240] per layer and the non-linear activation function between hidden layers is "tanh".

The primary dataset was generated by DP Generator (DP-GEN).[6] The initial structures that initiated the DP-GEN workflow were obtained through short-time molecular dynamics simulations. After accumulating approximately 3000 data points, we introduced enhanced sampling to the dynamics section of the DP-GEN workflow. We first focused on enhanced sampling for reaction R3, and as a result, a total of approximately 9000 structures with explicit solvent models were obtained during this phase of the DP-GEN workflow. Subsequently, we expanded the dataset by enhanced sampling molecular dynamics simulations for reactions R1 and R2. Ultimately, we obtained a comprehensive training set comprising 20,266 structures, including those representing the three distinct reactions. In the DP-GEN workflow, the training steps amounted to 500,000 iterations with a learning rate ranging from 10^{-3} to 10^{-8}. For the final model used in accuracy testing and subsequent applications, we trained it for 2,000,000 iterations.

Additional details of DP model validation

RDF

The Radial Distribution Functions (RDF) of atomic pairs in the water environment of *NNH species were obtained by statistical analysis of the 1 ps trajectory simulations of AIMD (PBE+D3)[7–9] and DPMD at 300 K in an NVT ensemble. Both simulations were initiated from an identical structure and propagated without any enhanced sampling techniques. A time step of 0.5 fs was employed, resulting in a total of 2000 steps.

Notably, this 1 ps duration is insufficient for the system to reach full equilibration, especially for atom pairs with strong interactions and low numbers, such as N_{top}-H. Therefore, this analysis focuses exclusively on the distributions of relatively abundant atom pairs, namely O-O, O-H, and H-H.

Energy and Force

The test set for the DP model contained three groups, which included configurations corresponding to three different reactions, respectively: Nitrogen adsorption on the catalyst (R1); Proton adsorption on the catalyst (R2); First hydrogenation step (R3) of nitrogen reduction reaction. For each group, configurations were taken every 1 ps over a 1 ns enhanced-sampling DPMD trajectory of the corresponding reaction at 300 K in an NVT ensemble. It is worth mentioning that for R2, some configurations collected in the aforementioned way were located at a very large s_d, which were far from the region of interest. Consequently, all configurations with s_d greater than 12 were manually excluded.

The resulting test set groups for R1, R2, and R3 comprise 835, 752, and 934 structures, respectively. For each structure in the test set, the single-point DFT calculation was performed and the obtained energies and forces were taken as references. The DP model performs well on the test set as we present in the main text.

Additional details of collective variables

The adsorption processes of H_2O and N_2 on the catalyst surface were described by $dO_{\min}$ and dN_{mean}, respectively. They are implemented in the following ways:

$$dO_{\min} = \frac{\beta}{\log \sum_i \exp\left(\frac{\beta}{s_i}\right)} \tag{S1}$$

$$dN_{\text{mean}} = \frac{\sum_i^2 d(\text{Ru} - \text{N}_i)}{2} \tag{S2}$$

The Voronoi CVs are used to describe the protonation states of atoms within a system.[10–12] Space is divided into Voronoi polyhedra, in which each hydrogen atom is assigned to a polyhedron centered around oxygen or nitrogen atoms. The goal is to count the number of hydrogen atoms associated with each oxygen or nitrogen atom. To count the number of H atoms n_i centered on O or N atom i, we use the formula:

$$n_i = \sum_{j=1}^{\text{Num1}} \frac{e^{-\lambda\left|R_i - R_j\right|}}{\sum_{\text{m=1}}^{\text{Num2}} e^{-\lambda\left|R_m - R_j\right|}} \tag{S3}$$

Num1 represents the hydrogen atoms that may participate in the reaction, and Num2 includes the possible bonding sites for these hydrogen atoms (including O, Ru, and N in our system). The parameter λ that controls the smoothness of the function is set to 5 during the dynamics calculations. By applying this formula, we determine the number of hydrogen atoms connected to each oxygen or nitrogen atom. This information helps to establish the protonation state of the corresponding atoms and further characterizes the ion distribution in the system. For example, if a Voronoi polyhedron contains 3 hydrogen atoms and 1 oxygen atom, it is identified as H_3O^+; a combination with only 1 hydrogen atom and 1 oxygen atom is labeled as OH^-. Subtracting specific values (subtracting 2 for oxygen and 1 for nitrogen) yields the "charge" used in our calculations, δ_i. Note that this "charge" is not obtained through traditional charge calculations.

In particular, we employ three Voronoi CVs, s_p, s_d, and s_{d2}, to represent the protonation state of the system, sum of distances between ions in the solution (excluding *NN and *NNH as ion pairs), and sum of distances between the reaction site N_{top} (as an ion) and ions in the solution. For s_d, and s_{d2}, positive (negative) values correspond to the separation distance of ions with opposite (same-sign) charges. More detailed descriptions of Voronoi CV refer to the cited references.[10–13]

$$s_p = \sum_{i=1}^{\mathrm{Num_O}} \delta_i + 2 \sum_{j=1}^{\mathrm{Num_{N\ or\ Ru}}} \delta_j \tag{S4}$$

$$s_d = \sum_{i \neq j}^{\mathrm{Num_O}} r_{i,j} \delta_i \delta_j \tag{S5}$$

$$s_{d2} = \sum_{i\ =1}^{\mathrm{Num_O}} r_{N_{\mathrm{top}},i} \delta_{N_{\mathrm{top}}} \delta_i \tag{S6}$$

Simulation of the first hydrogenation step of NRR with CV s_{d2}

For the first hydrogenation step of NRR (R3), the main text presents a free energy surface (FES) derived from a 10 ns molecular dynamics simulation employing enhanced sampling along the CVs s_p and s_d. In addition, a separate 10 ns enhanced-sampling MD simulation was conducted to better understand the approaching process of hydronium ion toward the adsorbed nitrogen molecule, along the single CV s_{d2}, which characterizes the separation of the hydronium ion and the adsorbed nitrogen molecule. The resulting one-dimensional FES is shown in Fig. S1. The configuration at $s_{d2} = 0$ corresponds to the structure [R3-b]. The region of $s_{d2} = 4 \sim 10$ Å roughly corresponds to [R3-a], and the decrease of s_{d2} from 4 to 10 Å shows the approaching of hydronium ion towards the adsorbed nitrogen molecule. A larger s_{d2} than 10 Å indicates water self-ionization reaction in the system.

As observed from Fig. S1, the free energy of the system progressively increases with the decrease of s_{d2} from 4 to 10 Å. The fully solvated hydronium ion ($s_{d2} \approx 10$ Å) in water is thermodynamically more stable (~ 0.1 eV) compared to the configuration where the hydronium ion is close to the adsorbed nitrogen molecule ($s_{d2} \approx 4$ Å), i.e., the process that the hydronium ion fully solvated in water approaches the adsorbed nitrogen molecule is endergonic with a small free energy change of 0.1 eV.

However, s_{d2} is not suitable for describing the first hydrogenation step in that the free energy changes precipitously in the region near [R3-b].

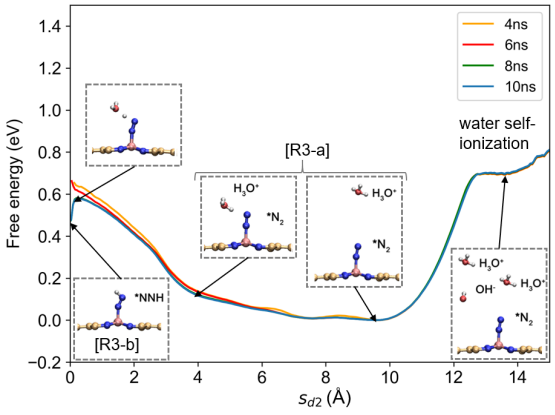

Figure S1: **One-dimensional projections of the FES of R3 along the s_{d2}.** $s_{d2} = 0$ corresponds to structure [R3-b], $s_{d2} = 4 \sim 10$ roughly corresponds to structure [R3-a], and a larger s_{d2} indicates that self-ionization of water occurs in the system. Key structures are marked, with other surrounding water molecules hidden.

Convergence test of the free energy surfaces

The evolution of the CVs over simulation time for the trajectories of the reactions discussed in the main text is depicted in Fig. S2, which supports the assertion of adequate sampling. Moreover, the convergence of the FES with respect to the simulation time was explicitly tested. As shown in Figs. S3–S5, these tests confirm that combined with

enhanced sampling, the 10 ns molecular dynamics simulations are sufficient to obtain converged free energy surfaces for all three reactions.

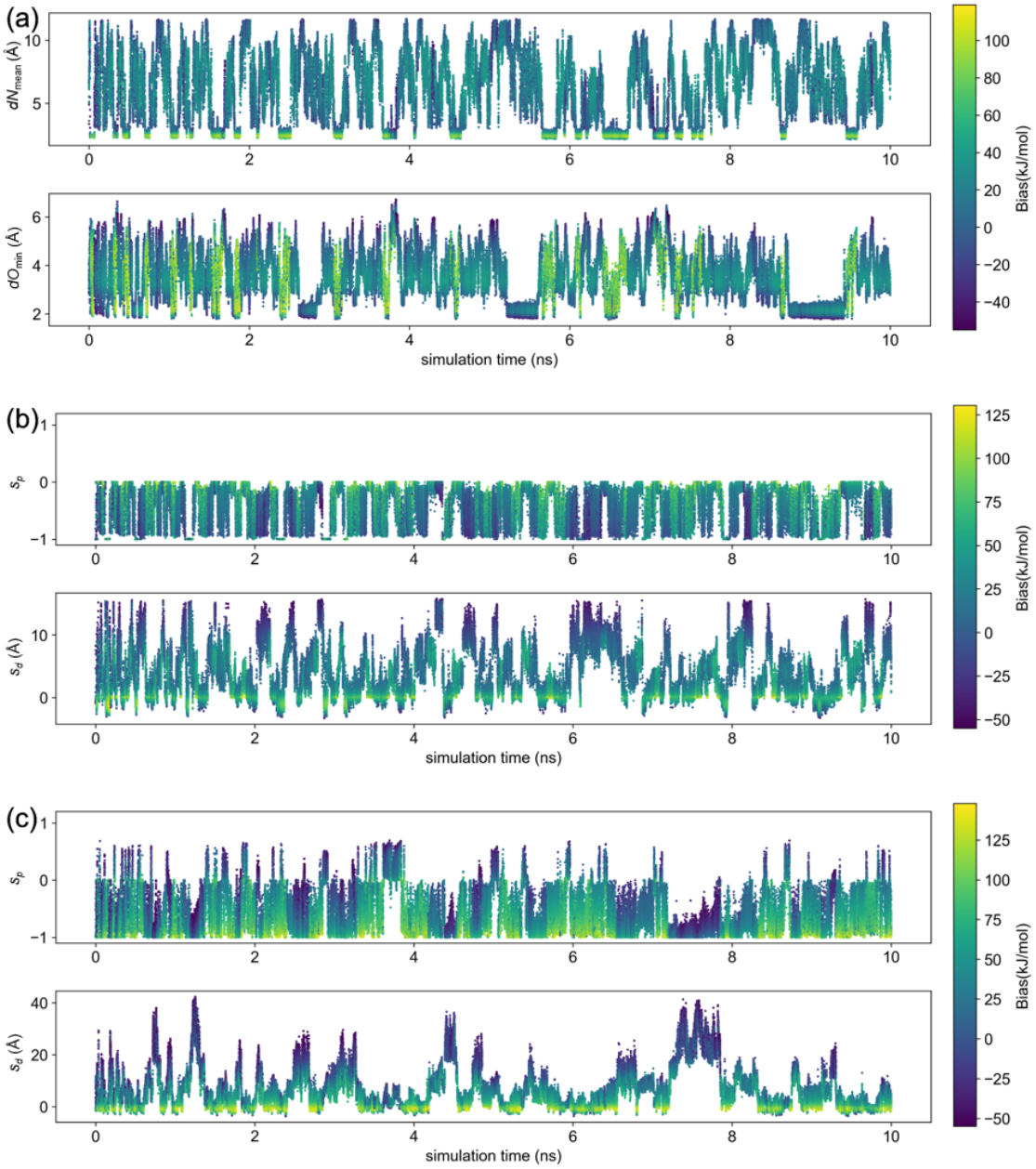

Figure S2: **The CV profiles for the trajectories. a**. Reaction R1; **b**. Reaction R2; **c**. Reaction R3.

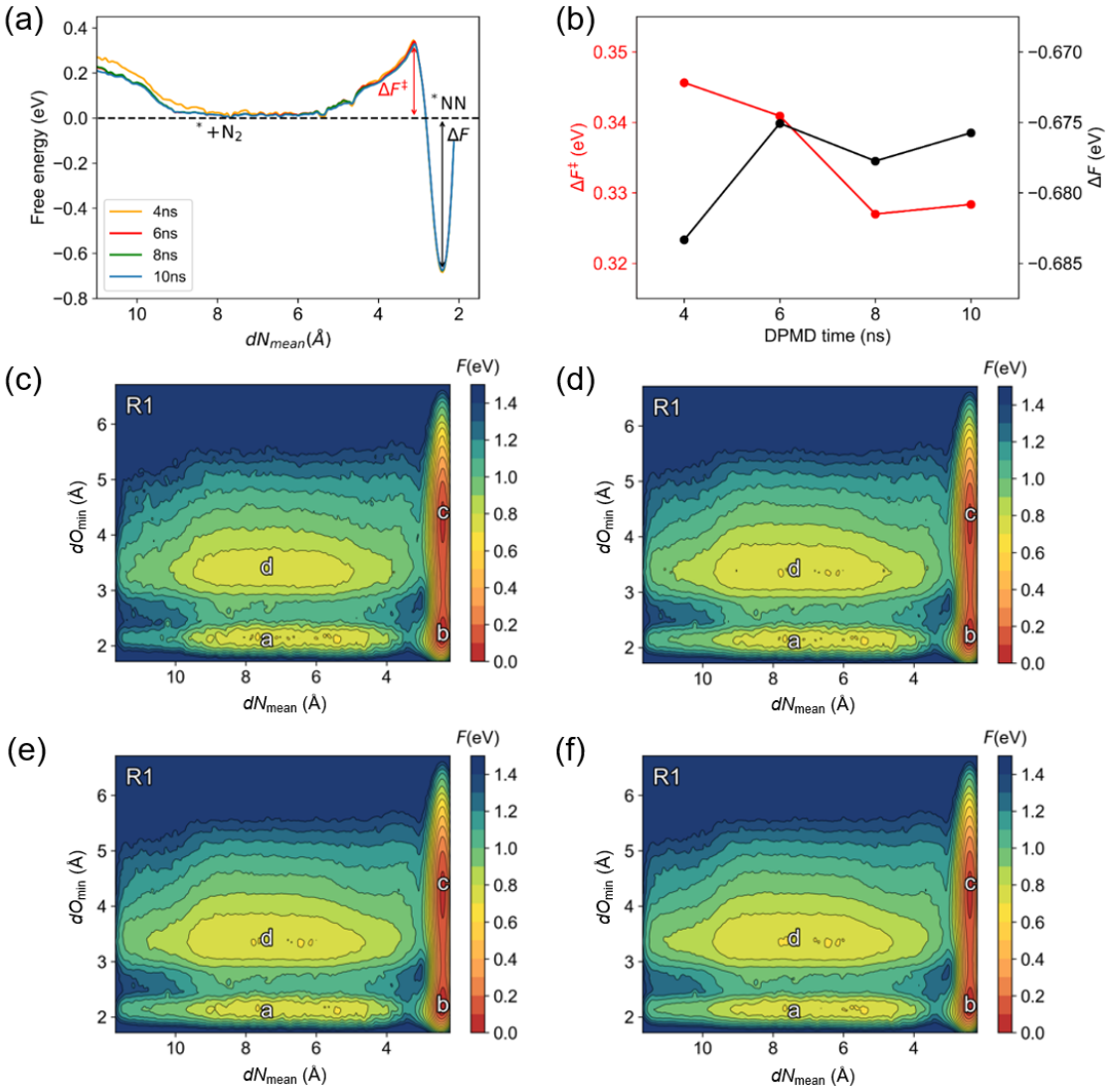

Figure S3: **Convergence of FES of reaction R1 over time. a**. Convergence test for the 1-dimensional free energy surface along dN_{mean}, in which $\Delta F^{\ddagger}$ denotes the free energy barrier, and ΔF denotes the free energy difference. The energy of the lowest point of the reactant (* + N_2) structure is set to 0. **b**. The free energy barrier and free energy difference obtained from DPMD simulations of different time lengths. **c,d,e,f**. Two-dimensional FES of R1 as a function of dO_{min} and dN_{mean}, corresponding to DPMD simulations of 4,6,8,10 ns length, respectively.

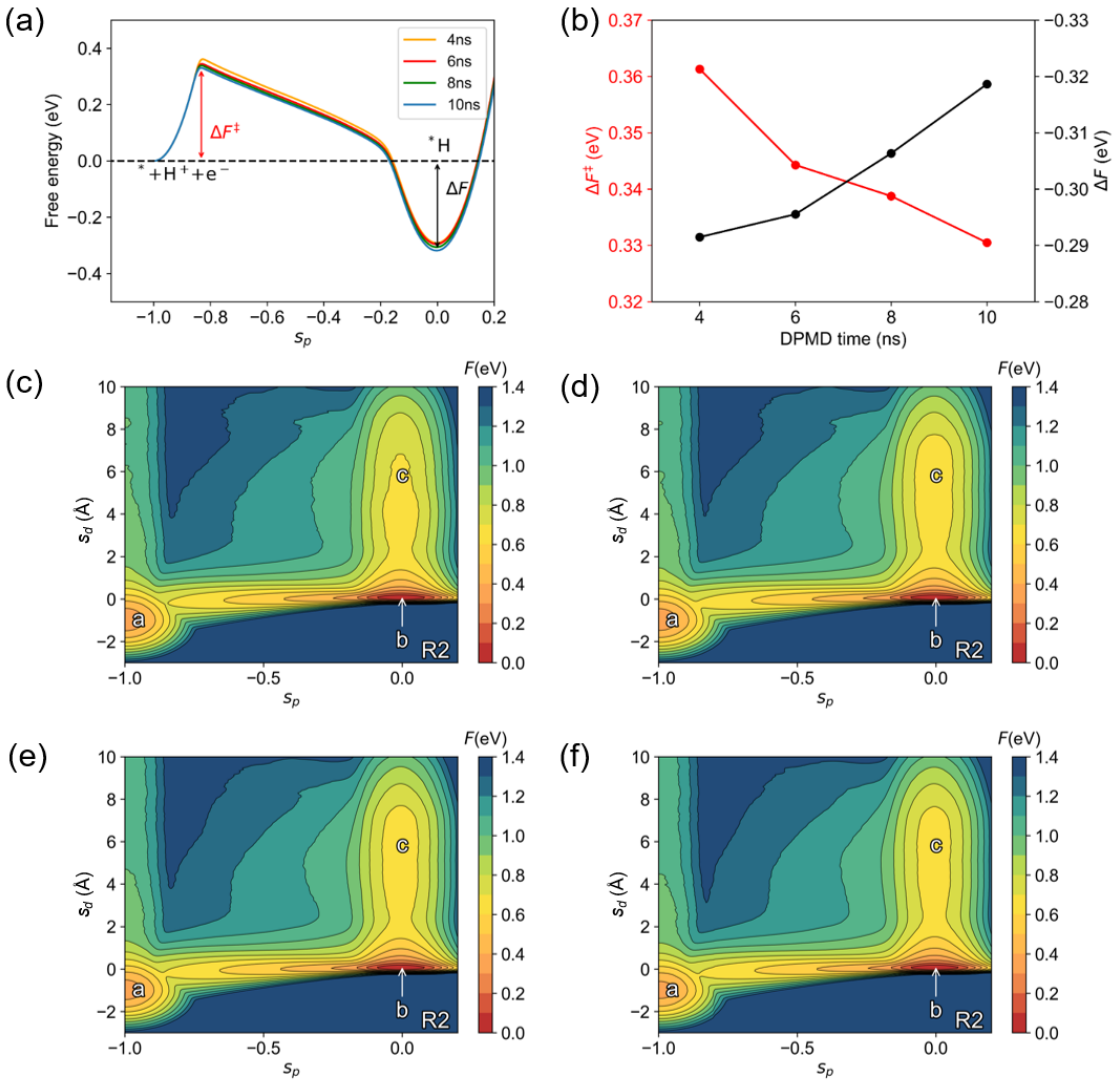

Figure S4: **Convergence of FES of reaction R2 over time. a**. Convergence test for the 1-dimensional free energy surface along s_p. The energy of the lowest point of the reactant (* + H^+ + e^-) structure is set to 0. **b**. The free energy barrier and free energy difference obtained from DPMD simulations of different time lengths. **c,d,e,f**. Two-dimensional FES of R2 as a function of s_p and s_d, corresponding to DPMD simulations of 4,6,8,10 ns length, respectively.

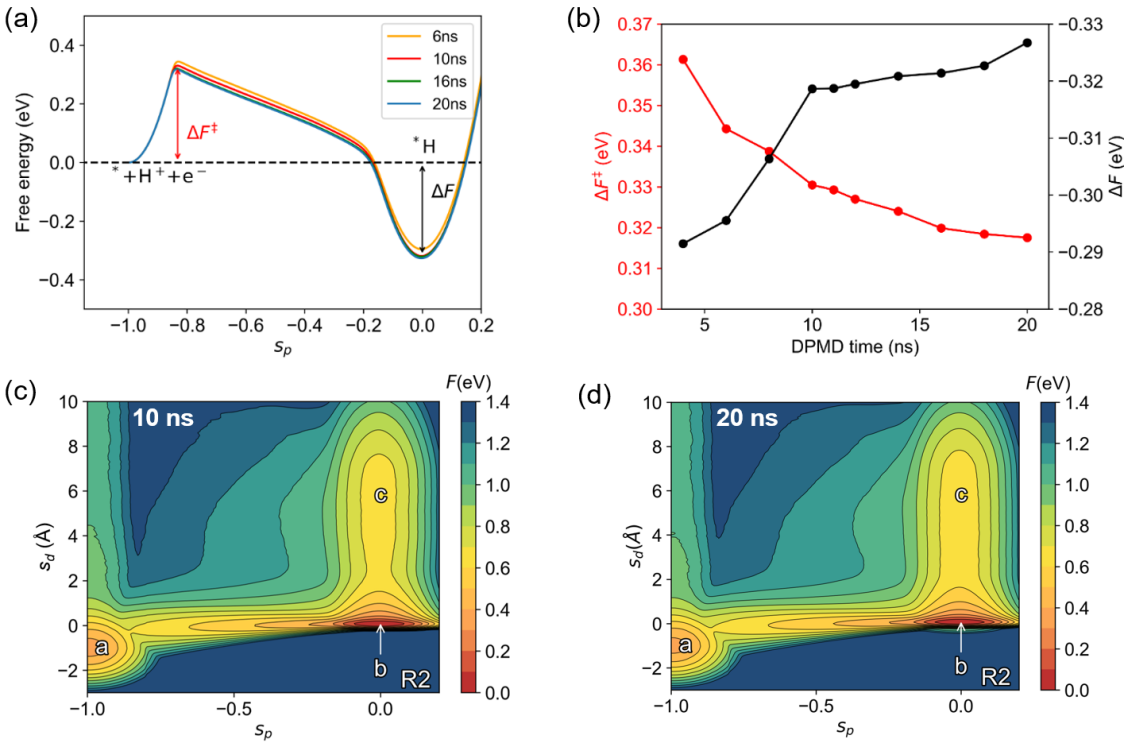

Figure S5: **Convergence of FES of reaction R2 over time. a**. Convergence test for the 1-dimensional free energy surface along s_p. The energy of the lowest point of the reactant ($* + H^+ + e^-$) structure is set to 0. **b**. The free energy barrier and free energy difference obtained from DPMD simulations of different time lengths. **c,d**. Two-dimensional FES of R2 as a function of s_p and s_d, corresponding to DPMD simulations of 10,20 ns length, respectively.

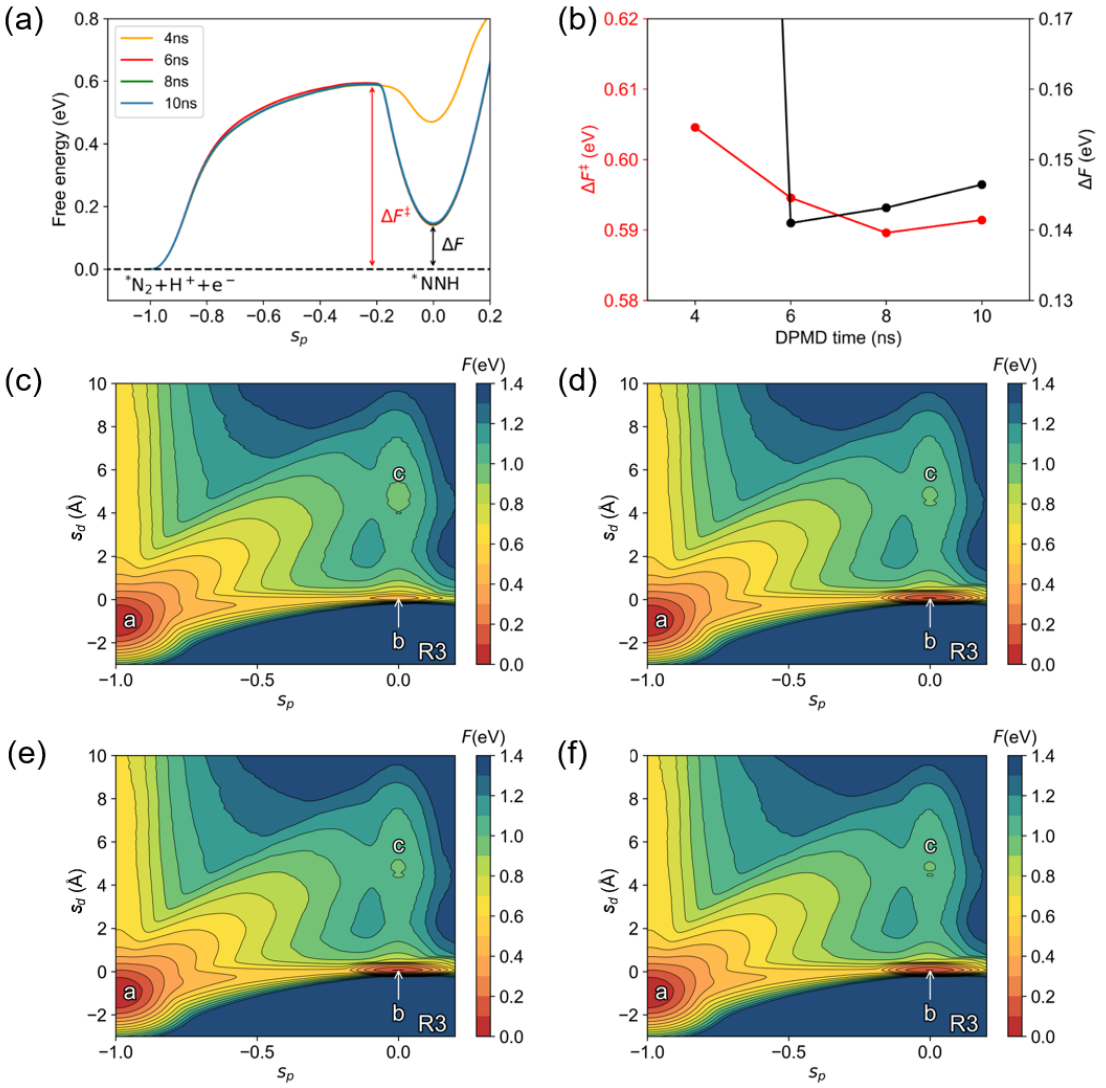

Figure S6: **Convergence of FES of reaction R3 over time.** **a**. Convergence test for the 1-dimensional free energy surface along s_p. The energy of the lowest point of the reactant ($^*N_2+H^+ + e^-$) structure is set to 0. **b**. The free energy barrier and free energy difference obtained from DPMD simulations of different time lengths. **c,d,e,f**. Two-dimensional FES of R3 as a function of s_p and s_d, corresponding to DPMD simulations of 4,6,8,10 ns length, respectively.

References

[1] Kühne, T. D.; Iannuzzi, M.; Del Ben, M.; Rybkin, V. V.; Seewald, P.; Stein, F.; Laino, T.; Khaliullin, R. Z.; Schütt, O.; Schiffmann, F.; others CP2K: An electronic structure and molecular dynamics software package-Quickstep: Efficient and accurate electronic structure calculations. *The Journal of Chemical Physics* **2020**, *152*.

[2] Peterson, A. A.; Abild-Pedersen, F.; Studt, F.; Rossmeisl, J.; Nørskov, J. K. How copper catalyzes the electroreduction of carbon dioxide into hydrocarbon fuels. *Energy & Environmental Science* **2010**, *3*, 1311–1315.

[3] Zhang, L.; Han, J.; Wang, H.; Saidi, W.; Car, R.; others End-to-end symmetry preserving inter-atomic potential energy model for finite and extended systems. *Advances in neural information processing systems* **2018**, *31*.

[4] Zhang, L.; Han, J.; Wang, H.; Car, R.; Weinan, E. Deep potential molecular dynamics: a scalable model with the accuracy of quantum mechanics. *Physical review letters* **2018**, *120*, 143001.

[5] Wang, H.; Zhang, L.; Han, J.; Weinan, E. DeePMD-kit: A deep learning package for many-body potential energy representation and molecular dynamics. *Computer Physics Communications* **2018**, *228*, 178–184.

[6] Zhang, Y.; Wang, H.; Chen, W.; Zeng, J.; Zhang, L.; Wang, H.; Weinan, E. DP-GEN: A concurrent learning platform for the generation of reliable deep learning based potential energy models. *Computer Physics Communications* **2020**, *253*, 107206.

[7] Perdew, J. P.; Burke, K.; Ernzerhof, M. Generalized gradient approximation made simple. *Physical review letters* **1996**, *77*, 3865.

[8] Grimme, S. Semiempirical GGA-type density functional constructed with a long-range dispersion correction. *Journal of computational chemistry* **2006**, *27*, 1787–1799.

[9] Grimme, S.; Antony, J.; Ehrlich, S.; Krieg, H. A consistent and accurate ab initio parametrization of density functional dispersion correction (DFT-D) for the 94 elements H-Pu. *The Journal of chemical physics* **2010**, *132*.

[10] Grifoni, E.; Piccini, G.; Parrinello, M. Microscopic description of acid–base equilibrium. *Proceedings of the National Academy of Sciences* **2019**, *116*, 4054–4057.

[11] Zhang, P.; Gardini, A. T.; Xu, X.; Parrinello, M. Intramolecular and Water Mediated Tautomerism of Solvated Glycine. *J. Chem. Inf. Model.* **2024**, *64*, 3599–3604.

[12] Zhang, P.; Xu, X. Modulation of Electric Field and Interface on Competitive Reaction Mechanisms. *J. Chem. Theory Comput.* **2025**, *21*, 6584–6593.

[13] Zhang, P.; Xu, X. Propensity of Water Self-Ions at Air(Oil)–Water Interfaces Revealed by Deep Potential Molecular Dynamics with Enhanced Sampling. *Langmuir* **2025**, *41*, 3675–3683.